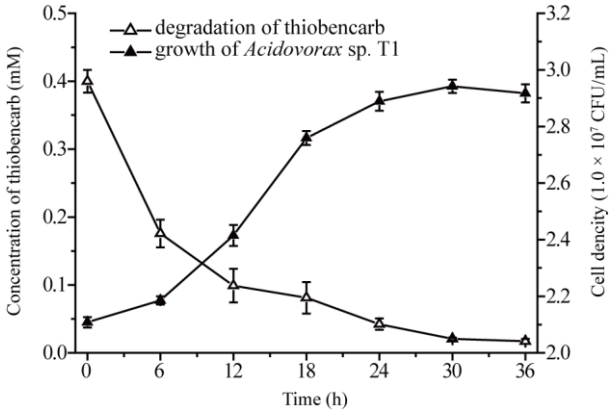

FIG. S1 Thiobencarb degradation and growth curve of strain T1. Strain was cultured in MSM supplemented with 0.4 mM thiobencarb as the sole sources of carbon, nitrogen and sulfur under aerobic conditions. The data are represented as the mean standard deviation for triplicate experiments.

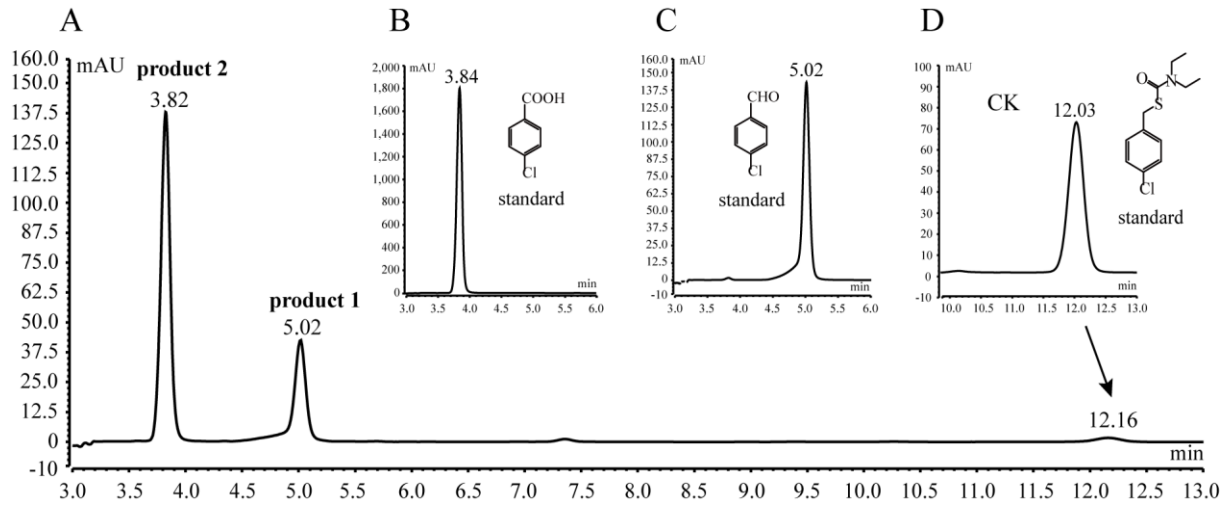

FIG. S2 HPLC analysis of the metabolites generated during thiobencarb degradation by *Acidovorax* sp. T1. (A) Metabolites of thiobencarb degradation; (B) standard 4CBA; (C) standard 4CDA; (D) CK, degradation negative control.

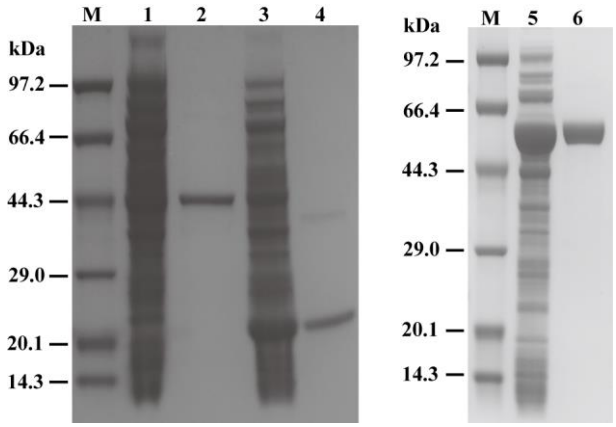

FIG. S3 SDS-PAGE analysis of the purified His_6-TmoA, His_6-TmoB and His_6-TmoC. Lane M: protein molecular weight Marker; lanes 1, 3, 5: crude extract of *E. coli* BL21 harboring pET-*tmoA*, pET-*tmoB* and pET-*tmoC*, respectively; lanes 2, 4, 6: purified His_6-TmoA, His_6-TmoB and His_6-TmoC, respectively.

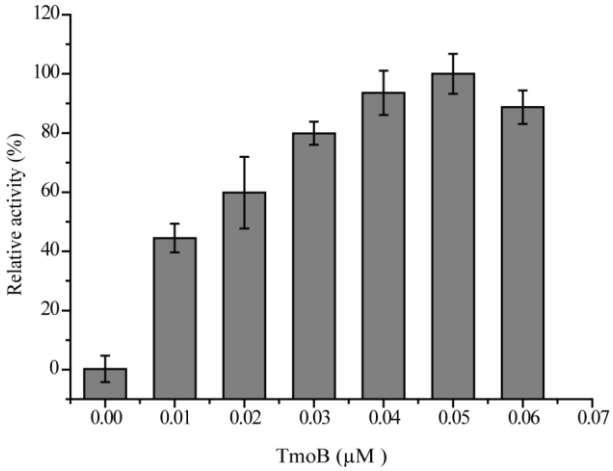

FIG. S4 Relationship between the activity of TmoAB against thiobencarb and various TmoA/TmoB molar ratios. The amount of TmoB was increased from 0-0.06 μM when the amount of TmoA was kept constant at 1 μM. The TmoA specific activity of 0.45 U mg^{-1} against thiobencarb was defined as 100% when 0.05 μM TmoB was added. The data are derived from three independent measurements, and errors bars indicate standard deviations.

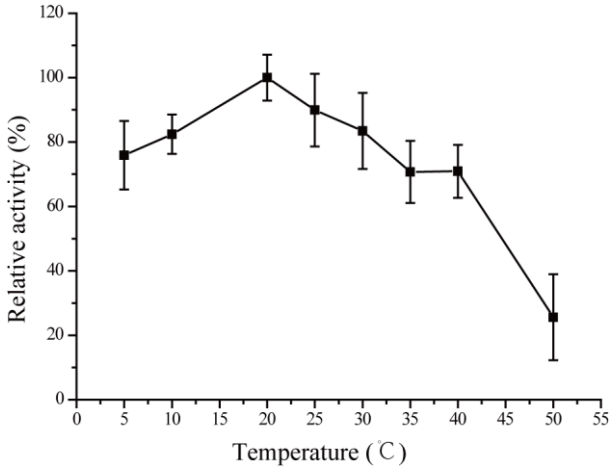

FIG. S5 Effects of temperature on TmoAB activity. TmoAB was incubated at pH 7.4 and different temperatures (5-50°C) for 60 min, and the relative activity was calculated by assuming that the activity observed at 20°C was 100%.

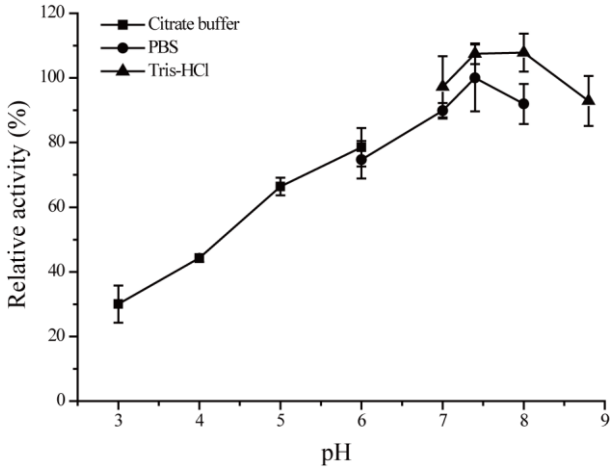

FIG. S6 Effects of pH on TmoAB activity. Three buffering systems: ■ 50 mM citrate buffer (pH 3.0 to 6.0), ● 50 mM PBS buffer (pH 6.0 to 8.0) and ▲ 50 mM Tris-HCl buffer (pH 7.0 to 8.8). The relative activity was calculated by assuming that the activity at pH 7.4 in PBS buffer was 100%.

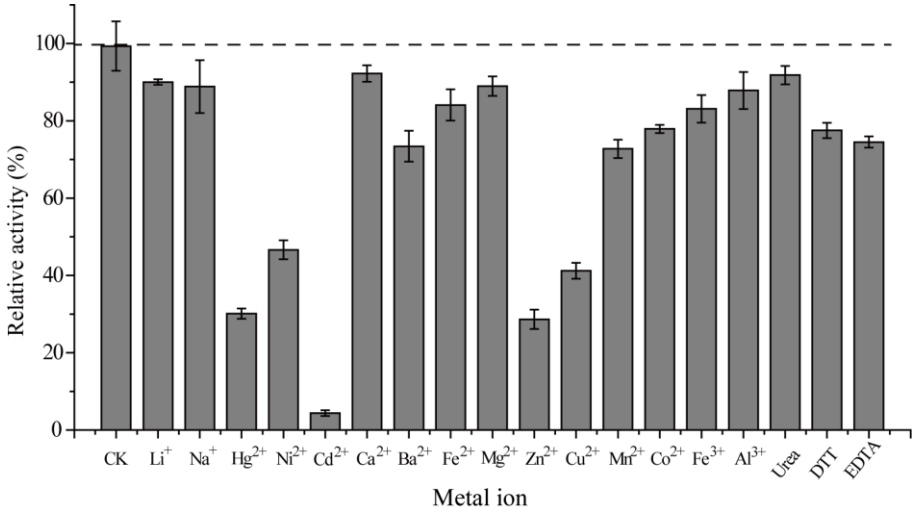

FIG. S7 Effects of metal ions and chemical agents on TmoAB activity. CK: control group without addition of any exogenous metal ions or compounds, and its relative activity was defined as 100%. The concentrations of urea, DTT and EDTA were 5 mM, and the concentrations of all metal ions were 1 mM.

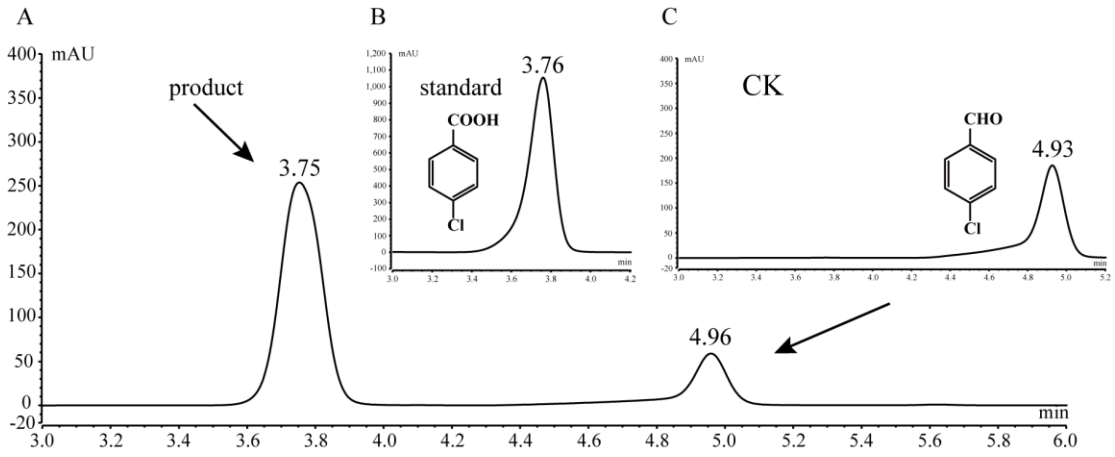

FIG. S8 HPLC analysis of the product generated during 4CDA conversion by TmoC. (A) Conversion product of 4CDA; (B) standard 4CBA; (C) CK, 4CDA negative control.

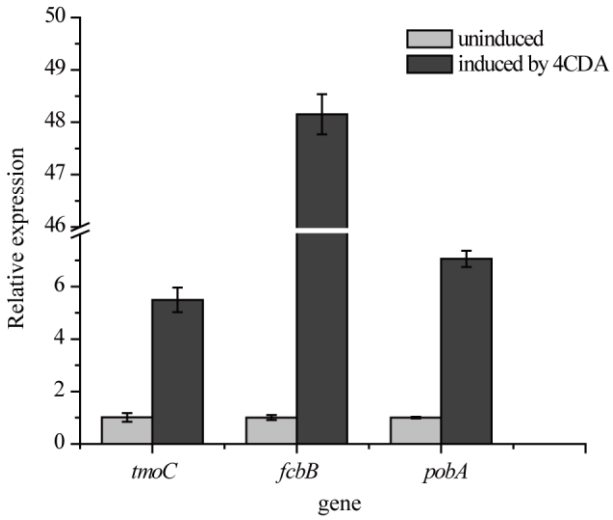

FIG. S9 Transcriptional levels of *tmoC, fcbB* and *pobA* in *Acidovorax* sp. T1 with or without 4CDA induction. Relative expression levels were calculated using the $2^{-\Delta\Delta CT}$ threshold cycle (C_T) method with 16S rRNA gene used as the reference gene. The data were derived from three independent measurements, and error bars indicate standard deviations.

A

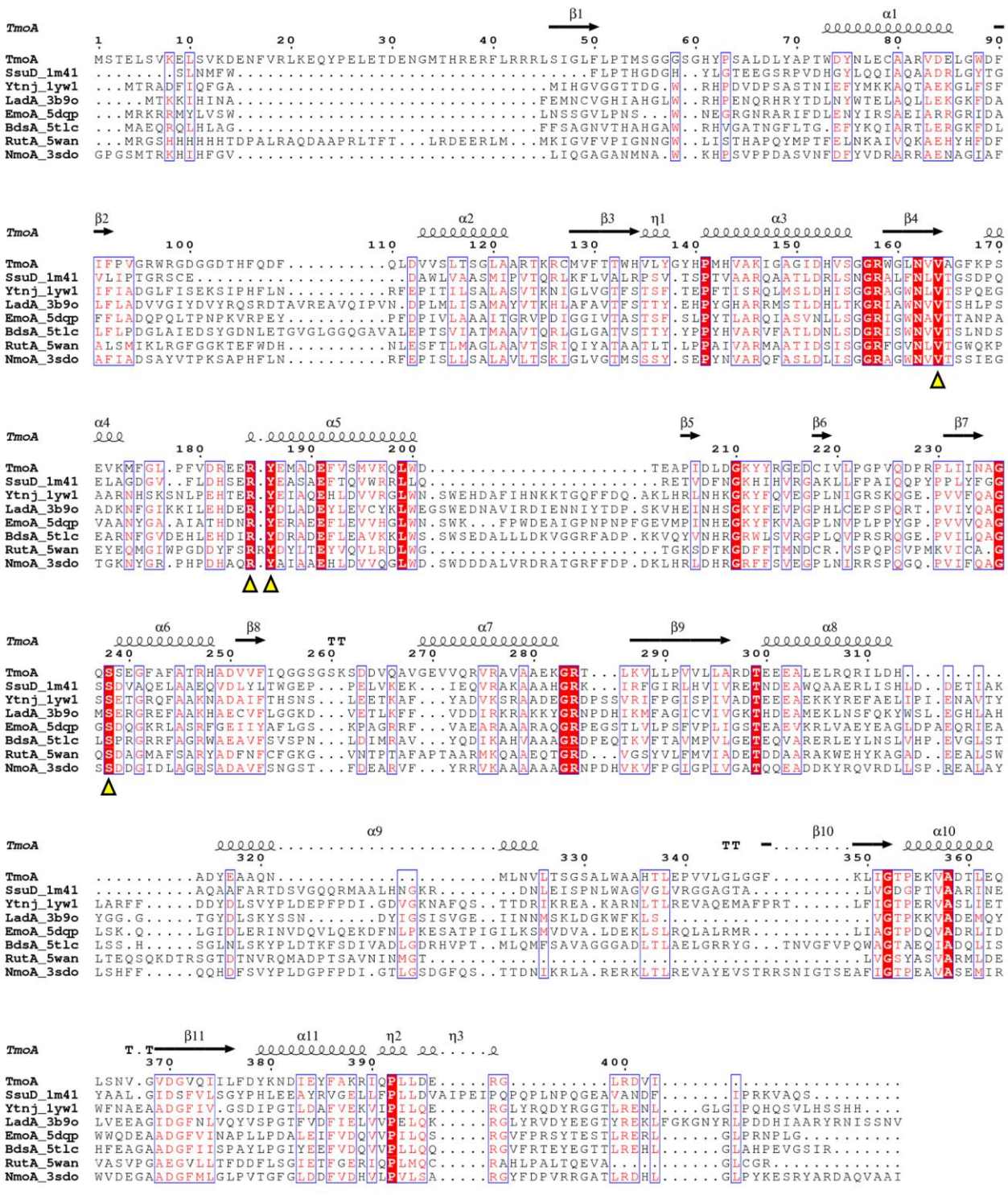
TmoA
SsuD_1m41
Ytnj_1yw1
LadA_3b9o
EmoA_5dqp
BdsA_5tlc
RutA_5wan
NmoA_3sdo

B

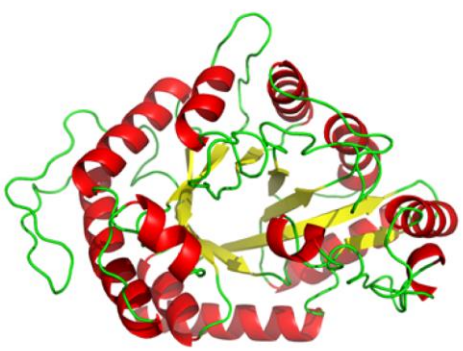

FIG. S10 Structure analysis of TmoA. (A) Sequence alignment of thiobencarb monooxygenase TmoA with the oxygenase components of several related two-component flavin-dependent monooxygenases. SsuD (PDB accession No: 1M41_A), alkanesulfonate monooxygenase from *Escherichia coli*; protein Ytnj (1YW1_A) from *Bacillus subtilis*; LadA (3B9O_A), alkane monooxygenase from *Geobacillus thermodenitrificans*; EmoA (5DPQ_A), EDTA monooxygenase from *Chelativorans* sp. BNC1; BdsA (5T1C_A), dibenzothiophene desulfurization enzyme A from *Bacillus subtilis*; RutA (5WAN_A), pyrimidine monooxygenase from *Escherichia coli*; NmoA (3SDO_A), nitrilotriacetate monooxygenase from *Burkholderia pseudomallei* 1710b. Numbers above the amino acid sequences indicate the residues' position of TmoA. The predicted TmoA secondary structure is shown above the alignment with α-helices, β-strands and turns. Conserved amino acids are shown in *boxes*, and identical amino acids are shown with a *red background.* The highly conserved residues (Val164, Arg185, Tyr186 and Ser238) labeled with yellow triangles are the predicted flavin binding sites of TmoA. (B) Tertiary structure prediction of thiobencarb monooxygenase TmoA with the oxygenase components of alkanesulfonate monooxygenase (1NQK.1) as a model. The construction of the structural model was carried out by SWISS-MODEL (https://www.swissmodel.expasy.org/), and the image further modified by software PyMOL.

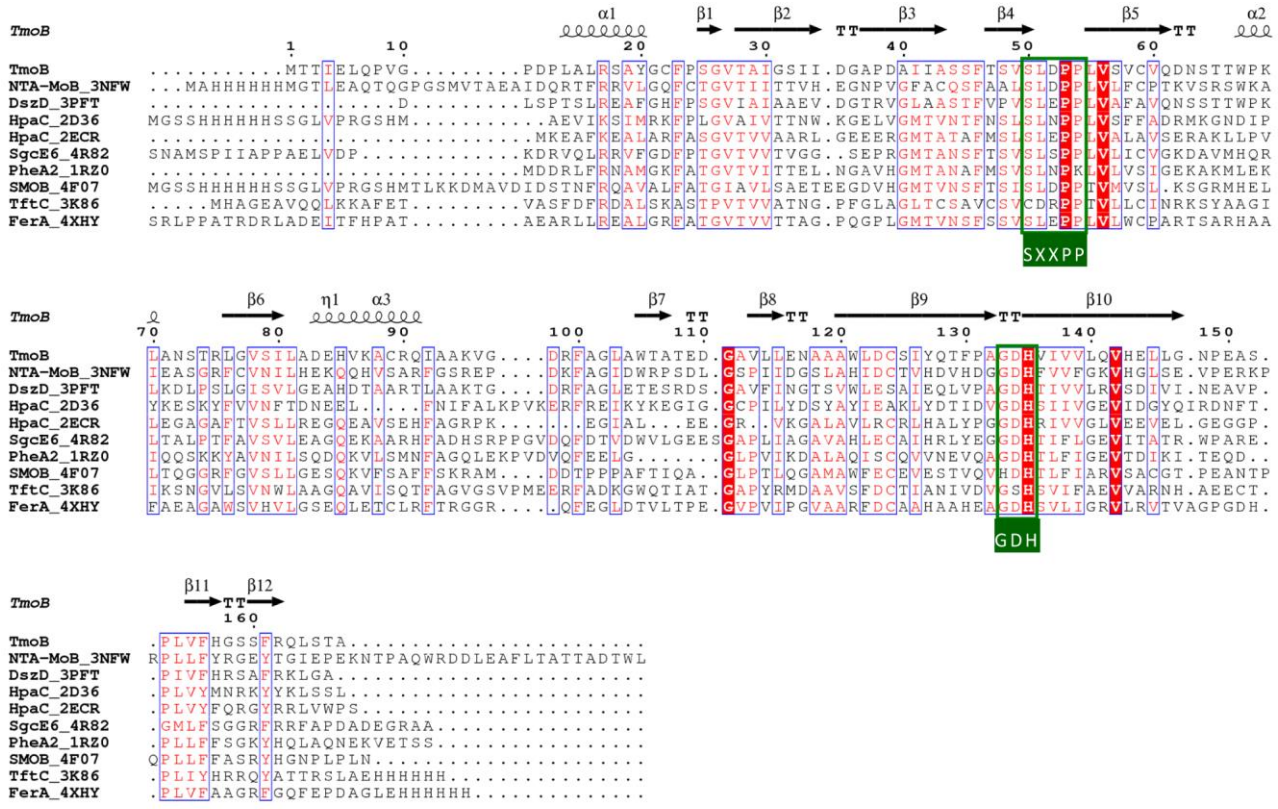

FIG. S11 Sequence alignment of TmoB and homologues. Abbreviations and PDB accession numbers are as following: NTA-MoB (PDB accession No: 3NFW_A), nitrilotriacetate monooxygenase component B from *Mycobacterium thermoresistibile* ATCC 19527; DszD (3PFT_A), flavin reductase from *Mycobacterium goodii*; HpaC (2D36_A), flavin reductase from *Sulfolobus tokodaii* str. 7; HpaC (2ECR_A), flavin reductase component of 4-hydroxyphenylacetate 3-monooxygenase from *Thermus thermophilus* HB8; SgcE6 (4R82_A), FAD oxidoreductase from *Streptomyces globisporus*; PheA2 (1RZ0_A), flavin reductase from *Parageobacillus thermoglucosidans*; SMOB (4F07_A), styrene monooxygenase flavin reductase from *Pseudomonas putida* S12; TftC (3K86_A), FAD oxidoreductase from *Burkholderia cepacia*; FerA (4XHY_A), FAD oxidoreductase from *Paracoccus denitrificans*. Numbers above the amino acid sequences indicate the residues'

position of TmoB. The predicted TmoB secondary structure is shown above the alignment with α-helices, β-strands and turns. Conserved amino acids are shown in *boxes*, and identical amino acids are shown with a *red background*. The regions highlighted in green are the conserved SXXPP and GDH motifs of HpaC-like flavin reductase subfamily.